Solar-Terrestrial Physics. 2026, vol. 12, iss. 1, pp. 50–58. DOI: 10.12737/stp-121202607. © 2026 S.N. Ponomarchuk, V.P. Grozov. Published by INFRA-M Academic Publishing House

DOI: 10.12737/stp-121202607
EDN: CGGDIT

Received June 27, 2025
Accepted September 22, 2025

TECHNIQUE OF IONOSPHERIC PARAMETER AUTOMATIC DETERMINATION USING DATA FROM VERTICAL SOUNDING WITH A CONTINUOUS CHIRP SIGNAL

S.N. Ponomarchuk
Institute of Solar-Terrestrial Physics SB RAS, Irkutsk, Russia, spon@iszf.irk.ru

V.P. Grozov
Institute of Solar-Terrestrial Physics SB RAS, Irkutsk, Russia, grozov@iszf.irk.ru

Abstract. We present a technique for determination of ionospheric parameters based on automatic interpretation of vertical sounding (VS) ionograms. Ionograms are interpreted using points with significant amplitude, which were detected after secondary data processing with results of modelling of VS signal height-frequency characteristic (HFC). We have developed algorithms to extract HFC tracks of signals reflected from the E, F1, and F2 layers. These algorithms involve analyzing signal amplitude characteristics and plotting distribution histograms of points falling into the HFC model mask when it is moved over the ionogram. The algorithm to detect tracks of signals reflected from sporadic layers is implemented separately. From the resultant VS HFC, we can estimate ionospheric parameters and calculate the electron density profile.

Keywords: radio wave propagation, ionospheric vertical sounding, ionogram, electron density profile, chirp signal.

INTRODUCTION

The method of ground-based vertical sounding of the ionosphere has not only retained its leading position in the ionosphere monitoring system, but has also practically become one of the main methods of diagnosing rapid dynamic processes, caused by the heliomagnetosphere-ionosphere coupling, in the upper atmosphere. Diagnostics of the ionosphere as a medium for HF radio wave propagation makes it possible to adapt radio systems of various types, including cognitive radio, to rapidly changing propagation conditions. Due to the sharply increased volume of experimental data obtained by SDR (Software-Defined Radio) ionosondes [Ivanov et al., 2019; Shindin et al., 2022; Kurkin et al., 2024], automation of secondary processing and interpretation of ionograms gains in importance. The main problem of automatic interpretation of ionograms is to determine ionospheric parameters and reconstruct the electron density profile. Approaches to solving this problem, put forward in numerous papers (see, e.g., the review in [Chen et al., 2018]), are generally linked to ionograms from real ionosondes.

The purpose of this work is to present a technique for automatically determining ionospheric parameters based on data from vertical sounding by a monostatic ionosonde with a chirp signal, which has been developed at the Institute of Solar-Terrestrial Physics SB RAS (ISTP SB RAS) [Podlesnyi et al., 2013; Kurkin et al., 2024].

The problems being solved involve secondary data processing, identification of recorded signals, construction of high-frequency characteristic (HFC) tracks, reconstruction of the electron density profile from HFC, and determination of ionospheric parameters.

Ionograms are interpreted at points with significant amplitude, identified during secondary data processing [Grozov et al., 2012; Penzin et al., 2019], using the results of HFC modeling of VS signals by the operational ionospheric model. Algorithms have been developed for isolating HFC tracks of signals reflected from the E, F1, and F2 layers of the ionosphere by analyzing amplitude characteristics of the signals and plotting histograms of points falling into the HFC model mask according to signal delay as it moves over the ionogram. An algorithm for identifying tracks of signals reflected from sporadic layers is implemented separately. The resultant VS HFC is used to determine ionospheric parameters and reconstruct the electron density profile.

IONOGRAM PROCESSING

Vertical sounding of the ionosphere is performed with a monostatic chirp ionosonde [Podlesnyi et al., 2013; Kurkin et al., 2024]. From the results of spectral analysis of the difference frequency signal, a VS ionogram is formed at the receiver output — the frequency dependence of signal group propagation time. In general, the recorded VS ionogram is an amplitude matrix $\tilde{A}_{nm}$. Each element of the matrix $\tilde{A}\left(f_i, h'_j\right), i=\overline{1,n},\ j=\overline{1,m},$ is defined by two characteristics — the virtual height of reflection h'_j and the frequency f_i. To select an array of points corresponding to the arrival time of signals with significant amplitude, secondary processing of the ionogram is carried out by filtering initial data and then compressing them by the cellular automaton method [Grozov et al., 2012; Penzin et al., 2019]. After secondary processing of VS ionogram, a new experimental point matrix $A\left(f_i, h'_j\right)$ is formed which matches the array of points with significant amplitude $\left(f, h', A\right)_k$, $k=\overline{1,M}$. The VS ionogram with the results of secondary data processing is presented in Figure 1. It has points with significant amplitude corresponding to the signals reflected singly from the F2 layer and singly ($1E_s$) and doubly ($2E_s$) from the E_s layer.

IONOGRAM INTERPRETATION

VS ionograms are automatically interpreted by analyzing selected points $A\left(f_i, h'_j\right)$ from the results of modeling of the height-frequency characteristic $h'\left(f\right)$, where f is the sounding frequency, using the operational semi-empirical ionospheric model. The HFC operational model developed at ISTP SB RAS is based on expansion of HFC nodal parameters — critical frequencies f_oE, f_oF1, f_oF2 and virtual heights h'F, h'F2, h_pF, h'F1 — with respect to natural orthogonal functions (NOF) [Dvinskikh, 1988]. The array of HFC nodal parameters was formed according to the empirical part of the semi-empirical ionospheric model developed at Irkutsk State University [Polyakov et al., 1986]. Each of the seven parameters that depends on local time t, month s, solar activity index F 10.7, and modified inclination X, is represented by triple expansion in EOF as

$$b\left(t, s, F, X\right) = \sum_{i=1}^{l_1}\sum_{j=1}^{l_2}\sum_{k=1}^{l_3} X_i\left(t\right) Y_{ij}\left(s\right) Z_{ijk}\left(F\right) V_{ijk}\left(X\right). \quad (1)$$

From the nodal parameters, monotonous HFC is reconstructed. F1- and F2-layer HFC is approximated by the quadratic function $h'\left(f\right) = af^2 + df + c.$ Polynomial coefficients are found from two pairs of nodal values of the function, assuming that the zero condition of the first derivative of the function is fulfilled at the first point of the layer. Then the expression for $h'(f)$ is written as

$$h'\left(f\right) = \frac{\left(f - f_1\right)^2}{\left(f_2 - f_1\right)^2}\left(h'_2 - h'_1\right) + h'_1, \quad (2)$$

where $\left(f_1, h'_1\right)$ and $\left(f_2, h'_2\right)$ stand for the beginning and end of the approximated layer. To calculate the E-layer HFC, we use the formula derived by converting the $N(h)$ profile, described by the parabola, to virtual heights.

$$h'\left(f\right) = \left(h_m\mathrm{E} - y_m\mathrm{E}\right) + \left(y_m\mathrm{E}/2\right)\left(f / f_o\mathrm{E}\right)\ln\frac{1 + f / f_o\mathrm{E}}{1 - f / f_o\mathrm{E}}, \quad (3)$$

where h_mE is the E-layer peak height; y_mE is the layer half-thickness; in the model, h_mE=120 km, y_mE=20 km.

Note that HFC can be calculated from the electron density profile $N(h)$ [Krasheninnikov, Lyannoi, 1991; Mikhailov, 2000; Vertogradov et al., 2018] by the predictive ionospheric model (e.g., [Bilitza et al., 2017]).

VS ionograms are interpreted as follows:

- amplitude characteristics are constructed for signals reflected from ionospheric layers;
- tracks and signals reflected from E and E_s layers are identified;
- location of signals reflected from the F1 and F2 layers is determined;
- the cutoff frequency of VS signal reflection and HFC control points are found;
- model masks for the F1 and F2 layers are constructed and their position in the ionogram is determined;
- the trace of ordinary component for signals reflected from the F1 and F2 layers are isolated and identified;
- VS HFC is formed and ionospheric layer parameters are defined.

Let us consider the process of interpreting an ionogram by this algorithm, using VS signal reflection from the two-layer ionosphere as an example (Figure 2). Predicted HFC $h'(f)$ is indicated by the blue line in Figure 2. At the first stage, we calculate the amplitude-height characteristic $\Psi\left(h'\right) = \sum_i A^2\left(f_i, h'_j\right)$. Summation is over points of the frequency range f_i for a fixed height h'_j. The characteristic $\Psi(h')$ averaged over ten points is denoted by the purple line. The first local maxima of the dependence $\Psi(h')$ define the height corridors of points with significant amplitude for signals reflected from the E and E_s layers.

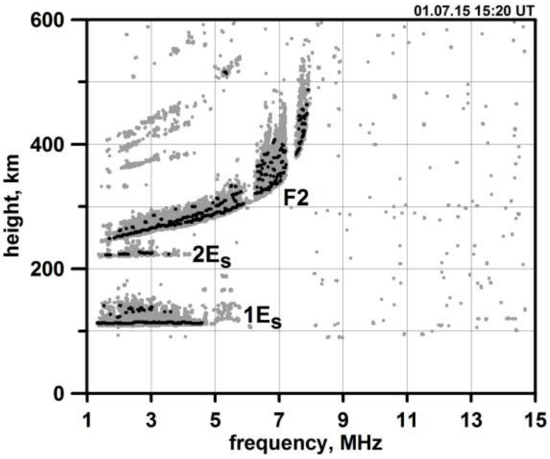

Figure 1. VS ionogram (gray dots) and secondary processing results (black dots)

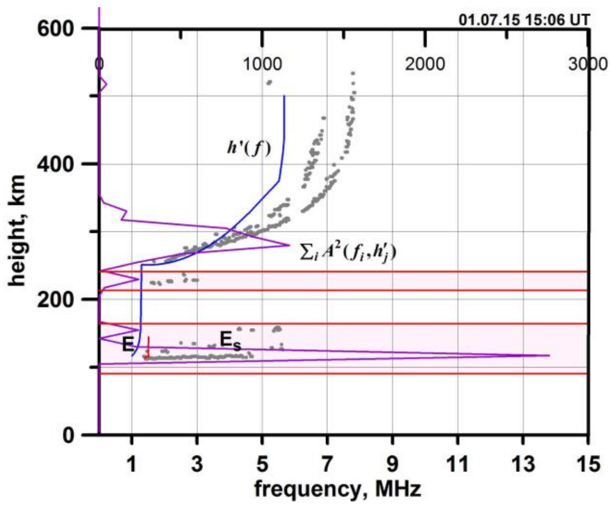

Figure 2. VS ionogram: processing results (gray dots); model mask (vertical red line); forecast of $h'(f)$ (blue line); amplitude-height characteristic (purple line)

These corridors are highlighted in pink. In the virtual height range from 90 to 160 km, the points are isolated which correspond to the arrival time of signals singly reflected from the E and E_s layers. Next, the frequency f_{mE} of the first local maximum is found in the selected array of points. A model mask is formed — a band of width Δh along the E-layer HFC in the frequency range from $\mu f_o^{pr}E$ to $f_o^{pr}E$, where $f_o^{pr}E$ is the predicted critical frequency of the E layer. Δh and μ can be varied depending on the delay resolution of the ionosonde and the frequency step. From the maximum number of points from the array $(f, h', A)_k$, $k = \overline{1, M}$, within the mask when it moves over the ionogram, the real critical frequency $f_o^{r}E$ is determined in a rectangle with boundaries $f \in \left[1, \max\left(f_o^{pr}E, f_{mE}\right) + 0.32\right]$ and $h \in [90, 160]$, and the E-layer HFC track is formed. If there are less than three points within the mask, $f_o^{r}E$ is taken equal to the predicted value of $f_o^{pr}E$ and the track fits the predicted E-layer HFC. From the remaining points with significant amplitude, a track of signals reflected from the E_s layer is formed. If there are signals doubly (or more) reflected from the E_s layer in the VS ionogram, they are also identified and tracks are found from $\Psi(h')$ maxima. Signals doubly reflected from the E_s layer in the ionogram shown in Figure 2 are identified in a rectangular band corresponding to the local maximum of the $\Psi(h')$ dependence and located at twice the height of the signal track with single reflection. Similarly, we can distinguish signal tracks with a large number of reflections from the E_s layer. The operational algorithm for determining parameters and identifying signal tracks reflected from the E and E_s layers has been implemented. Using the results of interpretation of signals reflected from the E_s layer, we find the height at which the ionogram is divided into regions of signal reflection from the E and F layers.

Figure 3 displays a VS ionogram without signals reflected from the E and E_s layers. In addition to the $\Psi(h')$

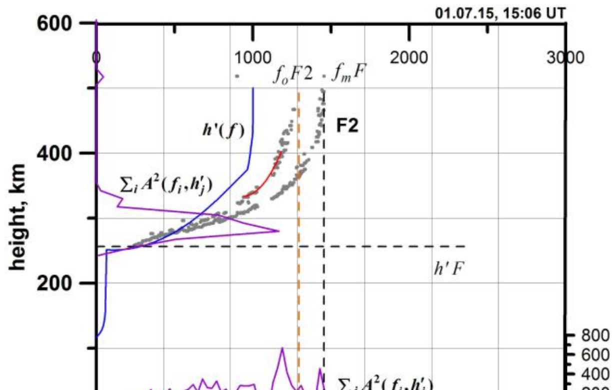

Figure 3. VS ionogram: processing results (gray dots); model mask (red line); forecast of $h'(f)$ (blue line); amplitude characteristics (purple lines)

characteristic, we calculate the amplitude-frequency characteristic $\Phi(f) = \sum_j A^2(f_i, h'_j)$. Summation is over the points of the height (time) sweep h'_j at a fixed frequency f_i; in this case, points with significant amplitude $(f, h', A)_k$, $k = \overline{1, M}$ are selected which are in the highlighted upper part of the ionogram according to the height of reflection. Figure 3 illustrates the amplitude-frequency characteristic $\sum_j A^2(f_i, h'_j)$ averaged over seven points.

From local extremes of the amplitude characteristics $\Psi(h')$ and $\Phi(f)$ we can determine control parameters of HFC tracks for signals in the ionogram. For example, the critical frequency of sounding signal reflection from the ionosphere f_mF is found from the zero level of $\Phi(f)$ and generally matches the critical frequency f_xF2 of reflection of the extraordinary signal component from the F2 layer in the absence of disturbances in the ionosphere. In Figure 3, f_mF is denoted by the black vertical dashed line. For f_mF, we can approximately define the F2-layer critical frequency: $f_oF2 = f_mF - f_H/2$, where f_H is the electron gyrofrequency. The algorithm uses f_H=1.5 MHz. In Figure 3, f_oF2 is indicated by the orange vertical dashed line. This method of determining f_oF2 allows us to run the operational algorithm of calculating the F2-layer critical frequency without further reconstruction of total HFC to identify F-layer parameters and to compute the electron density profile. The amplitude-height characteristic $\Psi(h')$ determines the F-layer minimum height $h'F$.

At the next stage, a model mask is constructed for the F2 layer — a band of width Δh along the predicted F-layer HFC (blue line in Figure 3) in the frequency range from $\beta f_o^{pr}F2$ to $f_o^{pr}F2$, where $f_o^{pr}F2$ is the predicted F2-layer critical frequency. From the maximum of the histogram of the number of points $(f, h', A)_k$, $k = \overline{1, M}$ falling into the model mask as it moves over the ionogram, its position in the ionogram is determined. An HFC track fragment for signals reflected from the F2 layer is constructed from the points within the model mask by approximating data with the least square technique. The approximating curve may not pass through the experimental points, but it is an approximation of the dependence under study and smooths out the outliers resulting from experimental errors. In Figure 3, this section of the track is depicted by the solid red line. To construct a complete HFC track of the F2 layer, the model track is continued up and down along the selected points with significant amplitude, using methods of continuous bonding or, in the absence of points, of extrapolation.

For the three-layer ionosphere, the algorithm for interpreting the ionogram is supplemented with the procedure for determining additional HFC control parameters from the amplitude characteristics $\Phi(f)$ and $\Psi(h')$: the F1-layer minimum height $h'F1$ and critical frequency f_oF1, points of local HFC minima (Figure 4). Determining the position of the model masks for the E, F1, and F2 layers in the ionogram from the control parameters allows us to confidently construct total HFC for the three-layer ionosphere.

IONOSPHERE PARAMETERS

As a result of VS ionogram interpretation, HFC *h'*(*f*) is formed for the E, F1, and F2 layers. Ionospheric parameters are determined from HFC: critical frequencies and minimum reflection heights for each ionospheric layer; minimum frequencies of reflection from the E and F2 layers. Additionally, when processing and interpreting the VS ionogram, the E_s-layer track is identified from which the critical frequency of the layer, the minimum reflection height, and shielding frequencies of the overlying ionospheric layers are found.

Figure 5 presents the results of determination of F1- and F2-layer critical frequencies for July 2, 2015. The sounding duty cycle was 1 min; and the scanning rate, 500 kHz/s. Relative errors were calculated to assess the reliability.

$$\delta = \frac{f_o^{\text{manual}} - f_o^{\text{a}}}{f_o^{\text{manual}}} \cdot 100\ \%,$$

where f_o^{manual}, f_o^{a} are the critical frequencies of the layer obtained due to manual and automatic processing of ionograms respectively. Figure 6 illustrates distributions of the relative error in determining the F1- and F2-layer critical

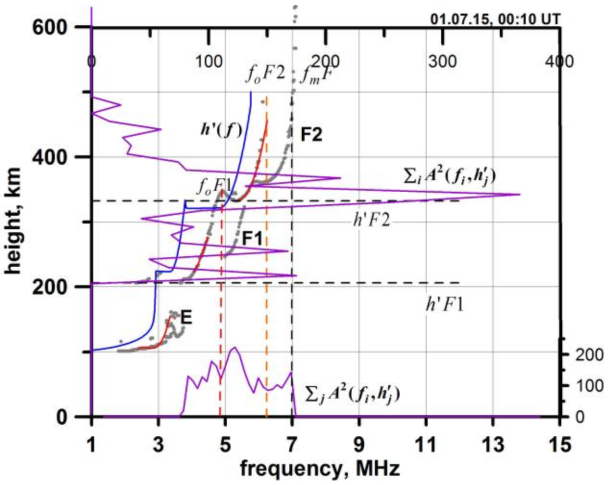

Figure 4. VS ionogram: processing results (gray dots); model masks (red solid lines); forecast of *h'*(*f*) (blue line); amplitude characteristics (purple lines)

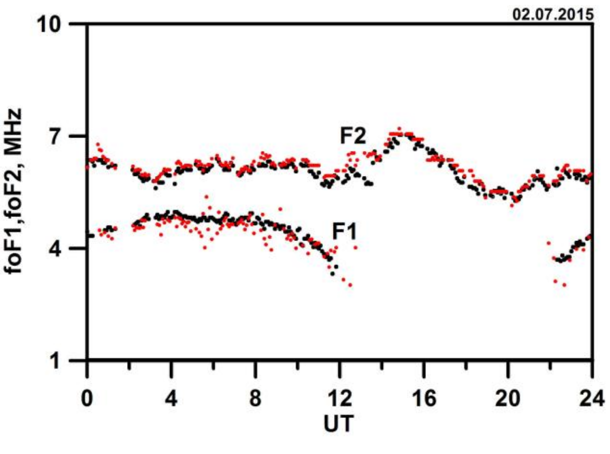

Figure 5. Results of determination of F1- and F2-layer critical frequencies for July 2, 2015: automatic processing (red dots), manual processing (black dots)

frequencies for July 2, 2015. The standard deviation of the relative errors in determining f_oF1 was 5 %; f_oF2, 2.7 %

The plasma frequency profile $f_e(h) = \sqrt{80.6N(h)}$ is also calculated from HFC. To reconstruct the vertical plasma frequency profile $f_e(h)$, a numerical solution of integral equations is used by modifying the Jackson method with increasing accuracy in the regions of maximum layers (subcritical frequencies) and valleys [Mikhailov, 2000]. From the $f_e(h)$ profile, additional F2-layer parameters are found: the F2-layer critical frequency f_oF2, peak height h_mF2, and coefficient *M(3000)* [Davis, 1973]. The results of identification of HFC of *h'*(*f*), calculation of the plasma frequency profile $f_e(h)$, and determination of the ionospheric layer parameters on July 1, 2015 at 15:06 UT and 00:10 UT for the two-layer and three-layer ionosphere are presented in Figures 7 and 8 respectively.

INTERPRETATION RESULTS

The developed algorithms were employed to implement the software package for automatic processing and interpretation of ionograms. The algorithms were validated based on vertical sounding data collected by the chirp ionosonde in different seasons of 2021 [Kurkin et al., 2024]. The sounding duty cycle was 15 s; and the scanning rate, 1000 kHz/s. Figure 9 presents the results of determination of the F2-layer critical frequency in January 2021. The difference between manual and automatic processing results is most pronounced for the local nighttime hours on January 15 when intense spread F was recorded (see Figure 9, *a*, 16 UT ionogram). Manual processing was performed in accordance with the URSI Handbook of Ionogram Interpretation and Reduction [URSI Handbook ..., 1977].

Figure 10 presents the results of manual and automatic processing of VS ionograms for different days in March 2021.

The greatest difficulties are caused by the processing of VS ionograms for the summer months of the year under conditions of the multilayer ionosphere and reflections from the E_s layer. Figure 11 shows the results of automatic ionogram processing in July 2021 when strong reflections from the E_s layer shielding the reflections of signals from the F-region were constantly recorded. The top left panel in Figure 11 illustrates daily variations in the E_s-layer critical frequency on July 1, 2021. As can be seen in the ionogram at 14:45 UT, the number of signal reflections from the E_s layer amounted to 5. In the middle and bottom left panels of Figure 11 are the results of determination of the F1- and F2-layer critical frequencies. The ionograms at 09:05 and 16:00 UT illustrate the possibilities of the developed interpretation algorithms for detecting reflections from the F-region in the presence of the E_s layer. The main errors in interpreting reflections from the F1 and F2 layers are related to the low signal-to-noise ratio in the high-speed mode of obtaining chirp ionograms. The recording duty cycle of ionograms is less than 1 min. The magnetoionic extraordinary component x for the signals reflected from the F2 layer has a small amplitude. During secondary processing, signals with the x component are eliminated relative to the signal-to-noise ratio, which leads to an error in determining the cutoff frequency of reflection from the F-region f_mF.

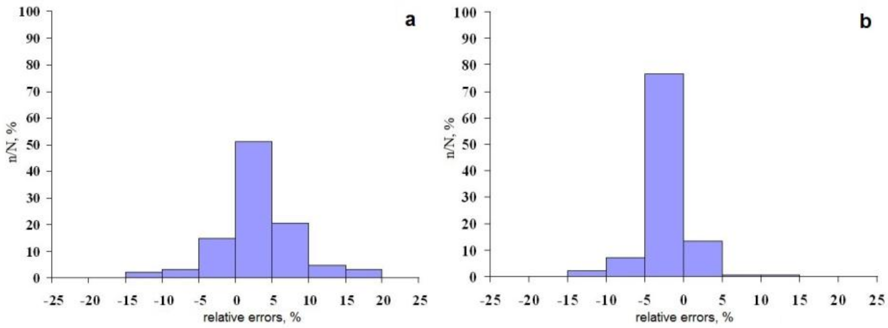

Figure 6. Distributions of relative errors in determining critical frequencies of the F1 (*a*) and F2 (*b*) layers for July 2, 2021

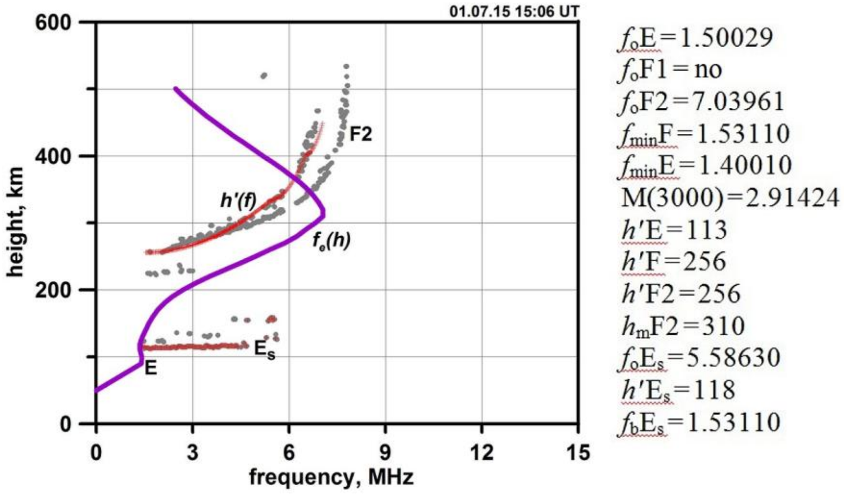

Figure 7. Ionospheric parameters (right) and processed VS ionogram on July 1, 2015 at 15:06 UT (left): results of secondary processing (gray dots); *h'*(*f*) and the E_s layer (red lines); plasma frequency $f_e(h)$ (purple line)

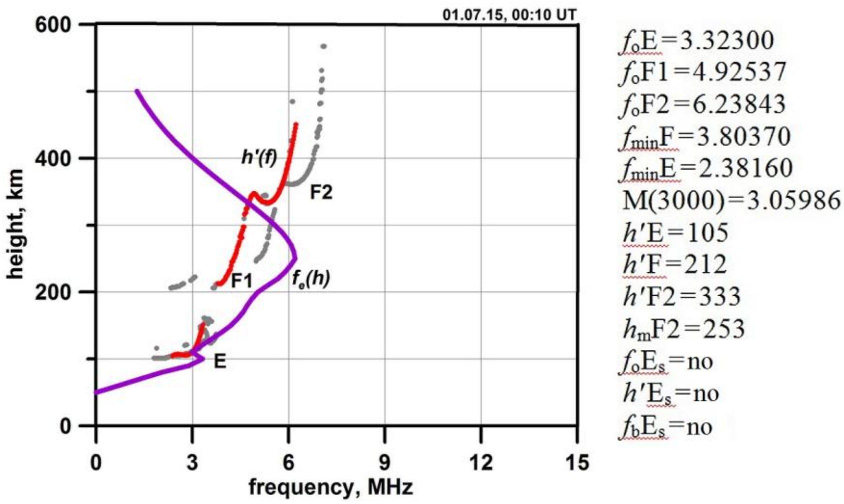

Figure 8. Ionospheric parameters (right) and the processed ionogram on July 1, 2015 at 00:10 UT (left): results of secondary processing (gray dots); *h'*(*f*) characteristic (red lines); plasma frequency $f_e(h)$ (purple line)

Figure 12 presents the results of determination of the critical frequency foF2 in October 2021.

Table lists the results of testing of the developed algorithms in different months of 2021 — standard deviations of relative errors in determining the Es-, F1-, and F2-layer critical frequencies. The general sample for each month contains at least 1200 ionograms.

Standard deviations of relative errors in determining critical frequencies (%)

Date	E_s	F1	F2
January 2021	–	–	6.6
March 2021	–	8.3	7.4
July 2021	7.2	12.2	7.5
October 2021	–	–	4.2

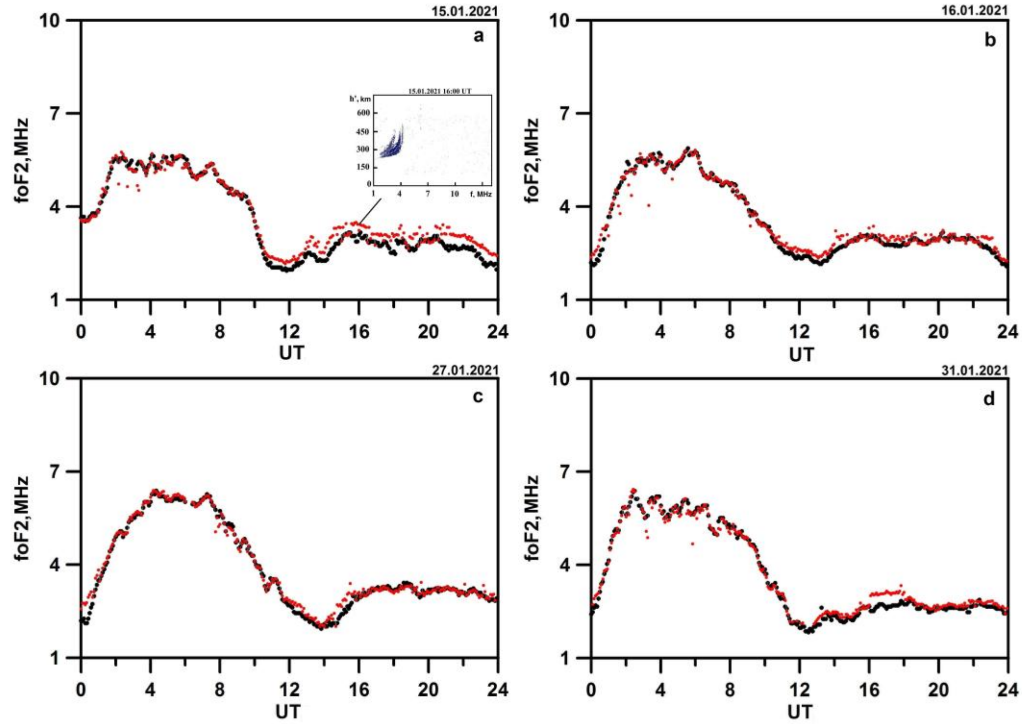

Figure 9. Results of determination of the F2-layer critical frequency in January 2021: automatic processing (red dots); manual processing (black dots)

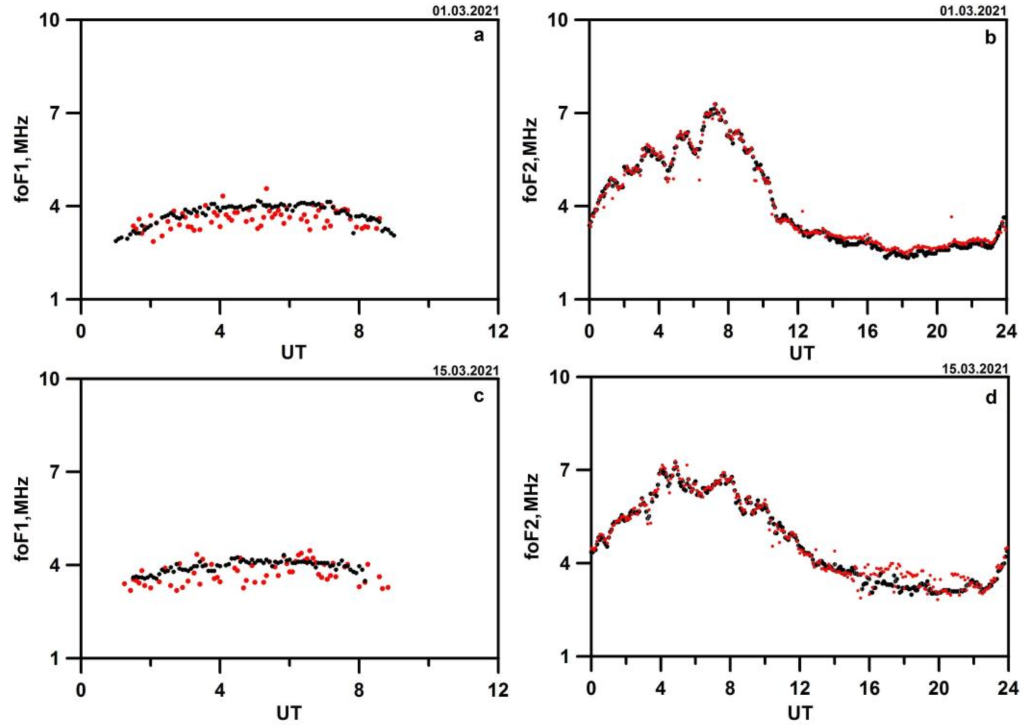

Figure 10. Results of determination of critical frequencies of the F1 (*a*, *c*) and F2 (*b*, *d*) layers on March 1 and 15, 2021: automatic processing (red dots); manual processing (black dots)

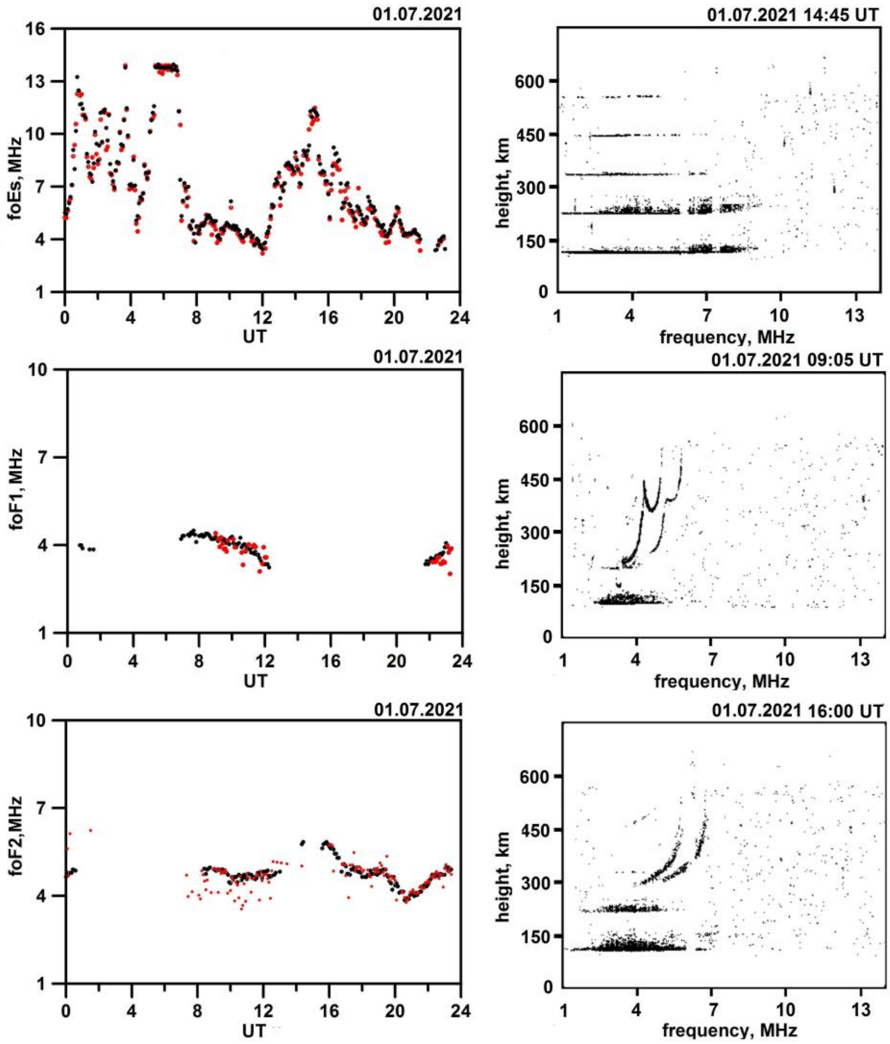

Figure 11. Results of determination of critical frequencies of the E_s, F1, and F2 layers (left, from top to bottom) according to VS ionograms at 09:05, 14:45, 16:00 UT (right, from top to bottom) on July 1, 2021: automatic processing (red dots), manual processing (black dots)

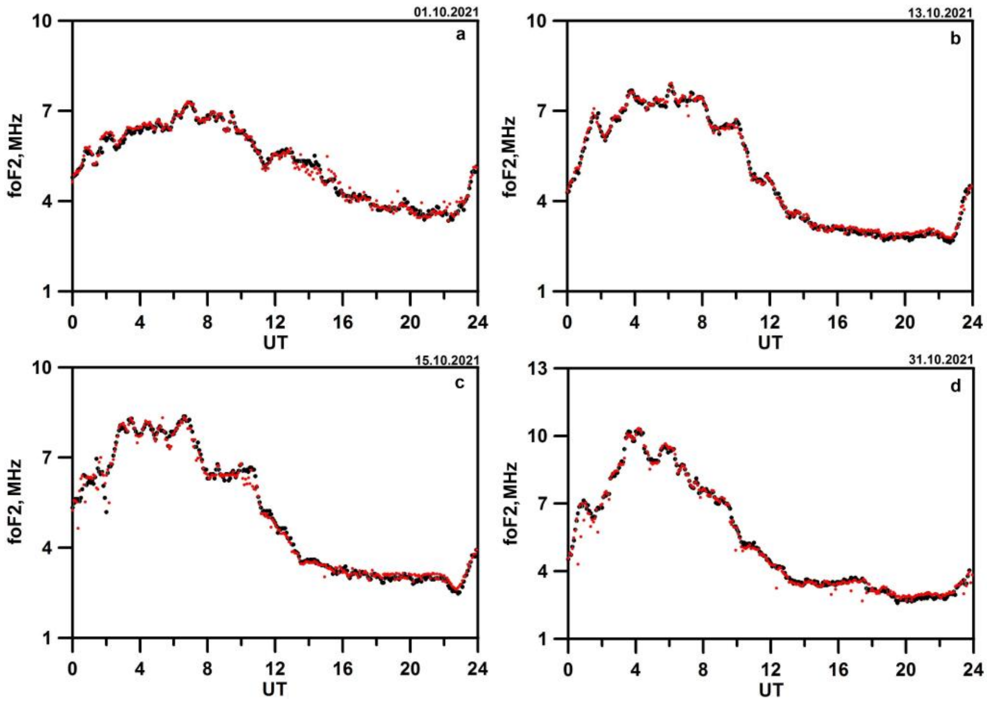

Figure 12. The same as in Figure 9 for October 2021

From the experience of using the software package for automatic processing and interpretation of VS ionograms under various heliogeophysical conditions, we can formulate recommendations for applying the package to chirp sounding of the ionosphere. It is recommended to use the software package in the following conditions:

1) there is no spot interference with a low signal-to-noise ratio;

2) there are no ionospheric disturbances caused by geomagnetic storms;

3) there are no traveling ionospheric disturbances leading to recording additional crescent-shaped signals in ionograms.

It is also recommended to use the software package for processing and interpreting VS ionograms of a stratified medium without off-angle reflections.

CONCLUSION

We have devised a technique of ionospheric parameter automatic determination from points with significant signal amplitude, identified during secondary processing of ionograms. We have developed algorithms for constructing tracks of signals reflected from ionospheric layers by analyzing amplitude characteristics of signals. As a result of VS ionogram interpretation, HFC $h'(f)$ is formed for the E, F1, and F2 layers. From VS HFC, the ionospheric parameters are determined and the vertical electron density profile is restored. Additionally, the E_s-layer track is identified. The software package for automatic processing and interpretation of vertical sounding ionograms with a continuous chirp signal has been implemented. The output characteristics of the package are critical frequencies and minimum reflection heights for each ionospheric layer, minimum frequencies of reflection from the E and F2 layers, F2-layer peak height and coefficient *M(3000)*, vertical plasma frequency profile. From the E_s-layer track, we found the critical frequency of the layer, the minimum reflection height, and the shielding frequency of the overlying ionospheric layers.

The greatest errors in determining ionospheric parameters during automatic processing of VS ionograms arise from

1) errors in predicting HFC tracks by ionospheric models;

2) false interpretation of the x component of the signal reflected from the F2 layer under multipath conditions of the recorded signal;

3) shielding of the F-region by the E_s layer in summer;

4) the presence of ionospheric irregularities during geomagnetic disturbances;

5) the presence of traveling ionospheric disturbances;

6) a low signal-to-noise ratio of recorded signals.

The developed algorithms can be employed to process large arrays of vertical sounding data to identify patterns and features of changes in the main parameters when analyzing ionospheric events. The developed software package can be an integral part of information systems for predicting HF radio wave propagation along paths equipped with ionospheric diagnostic tools.

The work was financially supported by the Ministry of Science and Higher Education of the Russian Federation (Subsidy No. 075-GZ/Ts3569/278). The experimental data was obtained using the equipment of Shared Equipment Center «Angara» [http://ckp-rf.ru/ckp/3056/].

REFERENCES

Bilitza D., Altadill D. Truhlik V., et al. International Reference Ionosphere 2016: From ionospheric climate to real-time weather predictions. *Space Weather*. 2017, vol. 15, iss. 2, pp. 418–429. DOI: 10.1002/2016SW001593.

Chen Z., Gong Z., Zhang F., Fang G. A new ionogram automatic scaling method. *Radio Sci*. 2018, vol. 53, iss. 9, pp. 1149–1164. DOI: 10.1029/2018RS006574.

Davies K. *Ionospheric Radio Waves.* London, Blaisdell, 1969, 460 p.

Dvinskikh N.I. Expansion of ionospheric characteristics fields in empirical orthogonal functions. *Adv. Space Res.* 1988, vol. 8, iss. 4, pp. 179–187. DOI: 10.1016/0273-1177(88)90238-4.

Grozov V.P., Ilyin N.V., Kotovich G.V., Ponomarchuk S.N. Software system for automatic interpretation of ionosphere sounding data. *Pattern Recognition and Image Analysis*. 2012, vol. 22, iss. 3, pp. 458–463. DOI: 10.1134/S1054661812030042.

Ivanov V.A., Ivanov D.V., Ryabova N.A., et al. Studying the parameters of frequency dispersion for radio links of different length using software-defined radio based sounding system. *Radio Sci*. 2019, vol. 54, iss. 1, pp. 34–43. DOI: 10.1029/2018RS006636.

Krasheninnikov I.V., Lyannoi B.E. On the interpretation of one type of travelling ionospheric disturbance from ionograms of vertical radio sounding. *Geomagnetizm i Aeronomiya*. [Geomagnetism and Aeronomy]. 1991, vol. 31, iss. 3, pp. 427–433. (In Russian).

Kurkin V.I., Medvedeva I.V., Podlesnyi A.V. Effect of sudden stratosphere warming on characteristics of medium–scale traveling ionospheric disturbances in the Asian region of Russia. *Adv. Space Res.* 2024, vol. 73, iss. 7, pp. 3613–3623. DOI: 10.1016/j.asr.2023.09.020.

Mikhailov S.Ya. Ambiguity of the reconstruction of plasma frequency profiles from a given height-frequency characteristic and their discernibility for oblique propagation of HF radio waves in an isotropic ionosphere. *Radiophysics and Quantum Electronics.* 2000, vol. 43, iss. 10, pp. 766–782.

Penzin M.S., Ponomarchuk S.N., Grozov V.P., Kurkin V.I. Real-time techniques for interpretation of ionospheric backscatter sounding data. *Radio Sci*. 2019, vol. 54, iss. 5, pp. 480–491. DOI: 10.1029/2018RS006656.

Podlesnyi A.V., Brynko I.G., Kurkin V.I., et al. Multifunctional chirp ionosonde for monitoring the ionosphere. *Geliogeofizicheskie issledovaniya* [Heliogeophys. Res.]. 2013, iss. 4, pp. 24–31. (In Russian).

Polyakov V.M., Sukhodolskaya V.E., Ivelskaya M.K., et al. *Poluempiricheskaya model' ionosfery dlya shirokogo diapazona geofizicheskikh uslovii* [Semi-empirical Model of the Ionosphere for a Wide Range of Geophysical Conditions]. Moscow, 1986, 139 p. (In Russian).

Shindin A.V., Moiseev S.P., Vybornov F.I., et al. The prototype of a fast vertical ionosonde based on modern software-defined radio devices. *Remote Sensing.* 2022, vol. 14, iss. 3, 547. DOI: 10.3390/rs14030547.

URSI Handbook of Ionogram Interpretation and Reduction 1972. Moscow, Nauka Publ., 1978, 342 p. (In Russian).

Vertogradov G.G., Uryadov V.P., Vybornov F.I., Pershin A.V. Modeling of decameter radio-wave propagation under conditions of a wave-like electron-density disturbance. *Radiophysics and Quantum Electronics*. 2018, vol. 61, iss. 6, pp. 407–417. DOI: 10.1007/s11141-018-9902-7.

URL: http://ckp-rf.ru/ckp/3056/ (accessed June 26, 2025)

Original Russian version: Ponomarchuk S.N., Grozov V.P., published in Solnechno-zemnaya fizika. 2026, vol. 12, iss. 1, pp. 55–63. DOI: 10.12737/szf-121202607.

How to cite this article

Ponomarchuk S.N., Grozov V.P. Technique of ionospheric parameter automatic determination using data from vertical sounding with a continuous chirp signal. *Sol.-Terr. Phys*. 2026, vol. 12, iss. 1, pp. 50–58. DOI: 10.12737/stp-121202607.